

Topological impact of a simple self-replication geometric structure with great application potential in vacuum pumping and photovoltaic industry

Running title: Topological impact of a simple self-replication geometric structure

Running Authors: Luo and Day

Xueli Luo ^{a)} and Christian Day

Karlsruhe Institute of Technology, Institute for Technical Physics, 76021 Karlsruhe, Germany

^{a)} Electronic mail: Xueli.Luo@kit.edu

Topological effects exist from a macroscopic system such as the universe to a microscopic system described by quantum mechanics. We show here that an interesting geometric structure can be created by the self-replication procedure of a square with an enclosed circle, in which the sum of the circles' area will remain the same but the sum of the circumference will increase. It is demonstrated by means of Monte Carlo simulations that these topological features have great impacts to the vacuum pumping probability and the photon absorption probability of the active surface. The results show significant improvement of the system performance and have application potential in vacuum pumping of large research facilities such as a nuclear fusion reactor, synchrotron and in photovoltaic industry.

I. INTRODUCTION

Topological features are related to the geometric structure of the system.¹ Square and circle are two of simple shapes in two dimensional geometry. Suppose there is one square with the length of side of a . First, one enclosed (inscribed) circle is put into the square and so the square is divided into four disconnected corners (spaces). In the second step, the original square is divided into four identical squares, and each with an enclosed circle. In the next steps, this one-to-four self-replication procedure (one-to-two in each dimension) just repeats, as shown in Figure 1.

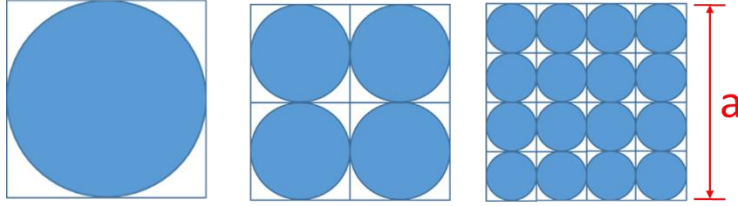


Fig. 1. The self-replication in the first steps from $N=1$ to $N=3$.

This self-replication procedure is under the constraint of the original square. In each step N , the number of circles M , the curvature κ of the circle, the number of the disconnected spaces χ , the total area of the circles A_o , and the total circumferences of the circles L are as follows.

$$M = 4^{N-1}, N = 1, 2, 3, \dots$$

$$\kappa = \frac{2^N}{a}, N = 1, 2, 3, \dots$$

$$\chi = (2^{N-1} + 1)^2, N = 1, 2, 3, \dots \quad (1)$$

$$A_o = \frac{1}{4}\pi a^2$$

$$L = 2^{N-1}\pi a, N = 1, 2, 3, \dots$$

These relations reveal two interesting topological features: (1) under the same constraint of the original two dimensional square, the zero dimensional and one dimensional measurements, such as the number of circles M , the number of the disconnected spaces χ and the circumference L could be unlimited; (2) the difference between bound and limit. Actually, the natural bound of area here is a^2 , but the total area of the circles is always unchanged as $A_o = \frac{1}{4}\pi a^2$ in each self-replication

step N . A self-replication may not be confused with a fractal process, e.g. the Wallis sieve, where smaller and smaller structures are generated while the big original structure remains.

This self-replication procedure could be easily extended to the three dimensional case, in which the original cube is filled with an enclosed (inscribed) sphere, and is divided into eight identical smaller cubes filled with smaller enclosed spheres in the next step (also one-to-two in each dimension), and so on. The number of spheres M , the curvature κ of the sphere, the number of the disconnected spaces χ , the total volume of the spheres V , and the total surface areas of the spheres A_o are given as follows.

$$\begin{aligned}
 M &= 8^{N-1}, N = 1, 2, 3, \dots \\
 \kappa &= \frac{2^N}{a}, N = 1, 2, 3, \dots \\
 \chi &= (2^{N-1} + 1)^3, N = 1, 2, 3, \dots \\
 V &= \frac{1}{6}\pi a^3 \\
 A_o &= 2^{N-1}\pi a^2, N = 1, 2, 3, \dots
 \end{aligned} \tag{2}$$

Astonishing enough is that the total volume of all spheres V is kept the same in each self-replication step as other measurements, such as the total surface areas of the spheres A_o are increasing. But please note that in different self-replication steps, neither the circles in two dimensional case nor the spheres in three dimensional case are the same since the curvatures of them, which are equal to the reciprocal of the radius in these two cases, become greater as N increases, and generally speaking, the curvature is an important physical parameter.²

In this paper, we will focus on the 2-D self-replication procedure and investigate its impact to the system performance by systematic Monte Carlo simulations.

II. PUMPING PROBABILITY

Usually, the requirement of the vacuum pumping is to provide high pumping speed for given gas load under the system geometric constraint. The essential topological features of the

aforementioned 2-D self-replication procedure are that the total circumferences of the circles will increase as the total areas of them is kept unchanged under the constraint of the original square. This provides us an opportunity to exploit the third dimension perpendicular to the plane. In the first step $N=1$, the original square is supposed to be an active pumping surface $A_s = a^2$ ($a = 200$ mm in simulation), and the enclosed circle is extended with a tube in the third dimension perpendicular to the plane as illustrated in Figure 2. As given in Eq. (1), the number of tubes M in the system will increase dramatically as N increases.

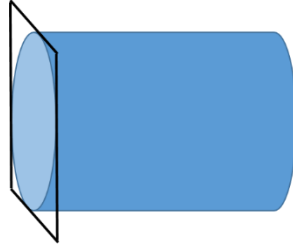


Fig. 2. The potential to exploit the dimension perpendicular to the plane in the first step $N=1$.

The configuration shown in Fig. 2 is similar to the typical configuration to connect a pump to a vacuum system, and the pumping speed S of the system is

$$S = \frac{1}{4}A_s \langle v \rangle w, \quad (3)$$

where $\langle v \rangle$ being the average velocity of the gas molecules in equilibrium, i.e. described by a Maxwell-Boltzmann distribution and w the pumping probability of the system.³ The particle flow rate corresponding to the known pumping speed S and particle density n is $Q=n \times S$. When $w=1$ in limit case, $Q = \frac{1}{4}A_s \langle v \rangle n$ correlates with the particle flux onto the surface A_s per unit time from one side. Please note the difference with the typical configuration to connect a pump to a vacuum system, where the wall of the facility is usually made of steel and has no pumping effect (zero pumping probability), and A_s in Eq. (1) will reduce to A_o , which is the inlet area of the pump.

In the free molecular flow regime, the pumping probability w of the system can be simulated by the Test Particle Monte Carlo (TPMC) simulation code such as Molflow+.⁴⁻⁵ In this

study we will use the code ProVac3D developed by ourselves, which has been used in different research projects and successfully parallelized.⁶⁻⁹ The length of the tube T_L is assigned to be $0.25a$, $0.5a$, $0.75a$, and a , respectively. Every tube includes the bottom. The sticking coefficient α of the original square, the tube wall and bottom is assigned to be 0.01 , 0.02 , and 0.03 , respectively. The reflection from the surface is assumed to be diffuse reflection. In order to distinguish the inlet from absorbing surfaces in the simulation, it is convenient to add a very short rectangular connection duct without pumping effect and with a length of 5 % to the length of side of the square is modelled as the reference case. In order to have precise simulation results, the simulations were carried out with 10^{12} or 10^{13} test particles on the supercomputer Marconi by using 640 to 16000 cores in parallel. The most important trick is to completely avoid the pseudo penetration of the test particles between adjacent tubes at their tangent point as a result of the inevitable numerical errors in the simulation.

Alternatively, the effective pumping probability w of this special system can be calculated by another method. When all tubes in each self-replication step N are independent and identical, the ratio of the total inlet area of all tubes to the area of the original square is always $\pi/4$, and w of the system for given α can be written as

$$w = k_1 w_{tube}(\alpha) + k_2 \alpha = \frac{1}{4} \pi w_{tube}(\alpha) + \left(1 - \frac{1}{4} \pi\right) \alpha, \quad (4)$$

with $w_{tube}(\alpha)$ being the pumping probability of each tube. In this way, the effect from the short duct will be automatically excluded and the simulation simplified since $w_{tube}(\alpha)$ is only dependent on the length to diameter ratio R in free molecular flow regime. The weighing factors $k_1 = \frac{\pi}{4}$ and $k_2 = 1 - k_1 = 1 - \frac{\pi}{4}$ represent ratios of the total opening area for the bundle of parallel tubes and the unchanged flat area to the area A_s of the original square, respectively.

The system has been simulated in both methods. Because they have very good agreement with each other, Table I only lists the simulation results in the first method that directly simulates

the system of M tubes. In the table, the total area of the tube walls is $A=L\times T_L$, with L given by Eq.

(1), R is the tube length to diameter ratio and $\delta = (w - \alpha)/\alpha$ is the relative increase of w .

TABLE I. Simulation results of the pumping probability w and corresponding relative increase δ .

	A	$\alpha=0.01$	δ	$\alpha=0.02$	δ	$\alpha=0.03$	δ
Reference case without tube	-	0.0099995(1)	-	0.0199979(1)	-	0.0299950(2)	-
N=1, M=1							
$T_L = 0.25a$, $R = 0.25$	$0.25\pi a^2$	0.0176834(1)	0.77	0.0350338(2)	0.75	0.0520623(2)	0.74
$T_L = 0.5a$, $R = 0.5$	$0.5\pi a^2$	0.0252246(2)	1.52	0.0495230(2)	1.48	0.0729504(3)	1.43
$T_L = 0.75a$, $R = 0.75$	$0.75\pi a^2$	0.0325844(2)	2.26	0.0633354(2)	2.17	0.0924177(3)	2.08
$T_L = a$, $R = 1$	πa^2	0.0397386(2)	2.97	0.0764066(3)	2.82	0.1103776(3)	2.68
N=2, M=4			--		--		--
$T_L = 0.25a$, $R = 0.5$	$0.5\pi a^2$	0.0252242(2)	1.52	0.0495221(2)	1.48	0.0729484(3)	1.43
$T_L = 0.5a$, $R = 1$	πa^2	0.0397382(2)	2.97	0.0764045(3)	2.82	0.1103745(3)	2.68
$T_L = 0.75a$, $R = 1.5$	$1.5\pi a^2$	0.0533535(2)	4.34	0.1001795(3)	4.01	0.1417082(3)	3.72
$T_L = a$, $R = 2$	$2\pi a^2$	0.0659539(2)	5.60	0.1207281(3)	5.04	0.1671916(4)	4.57
N=3, M=16			--		--		--
$T_L = 0.25a$, $R = 1$	πa^2	0.0397377(2)	2.97	0.0764029(3)	2.82	0.1103696(3)	2.68
$T_L = 0.5a$, $R = 2$	$2\pi a^2$	0.0659517(2)	5.60	0.1207229(3)	5.04	0.1671816(4)	4.57
$T_L = 0.75a$, $R = 3$	$3\pi a^2$	0.0878825(3)	7.79	0.1526880(4)	6.63	0.2032740(4)	5.78
$T_L = a$, $R = 4$	$4\pi a^2$	0.1054788(3)	9.55	0.1744451(4)	7.72	0.2248321(4)	6.49
N=4, M=64			--		--		--
$T_L = 0.25a$, $R = 2$	$2\pi a^2$	0.0659499(2)	5.59	0.1207172(3)	5.04	0.1671684(4)	4.57
$T_L = 0.5a$, $R = 4$	$4\pi a^2$	0.1054738(3)	9.55	0.1744316(4)	7.72	0.2248102(4)	6.49
$T_L = 0.75a$, $R = 6$	$6\pi a^2$	0.1294845(3)	11.95	0.1978406(4)	8.89	0.2443646(4)	7.15
$T_L = a$, $R = 8$	$8\pi a^2$	0.1428353(3)	13.28	0.2072730(4)	9.36	0.2506654(4)	7.36
N=5, M=256			--		--		--
$T_L = 0.25a$, $R = 4$	$4\pi a^2$	0.1054677(3)	9.55	0.1744155(4)	7.72	0.2247836(4)	6.49
$T_L = 0.5a$, $R = 8$	$8\pi a^2$	0.1428258(3)	13.28	0.2072512(4)	9.36	0.2506330(4)	7.35
$T_L = 0.75a$, $R = 12$	$12\pi a^2$	0.1535976(4)	14.36	0.2124475(4)	9.62	0.2533544(4)	7.45
$T_L = a$, $R = 16$	$16\pi a^2$	0.1564760(4)	14.65	0.2132812(4)	9.66	0.2536744(4)	7.46
N=6, M=1024			--		--		--
$T_L = 0.25a$, $R = 8$	$8\pi a^2$	0.1428146(3)	13.28	0.2072276(4)	9.36	0.2505976(4)	7.35
$T_L = 0.5a$, $R = 16$	$16\pi a^2$	0.1564627(4)	14.65	0.2132569(4)	9.66	0.2536379(4)	7.45
$T_L = 0.75a$, $R = 24$	$24\pi a^2$	0.1574424(4)	14.74	0.2134294(4)	9.67	0.2536910(4)	7.46
$T_L = a$, $R = 32$	$32\pi a^2$	0.1575207(4)	14.75	0.2134377(4)	9.67	0.2536922(4)	7.46
N=7, M=4096			--		--		--
$T_L = 0.25a$, $R = 16$	$16\pi a^2$	0.1564512(4)	14.65	0.2132341(4)	9.66	0.2536054(4)	7.45
$T_L = 0.5a$, $R = 32$	$32\pi a^2$	0.1575081(4)	14.75	0.2134155(4)	9.67	0.2536608(4)	7.46
$T_L = 0.75a$, $R = 48$	$48\pi a^2$	0.1575164(4)	14.75	0.2134161(4)	9.67	0.2536603(4)	7.46
$T_L = a$, $R = 64$	$64\pi a^2$	0.1575167(4)	14.75	0.2134157(4)	9.67	0.2536606(4)	7.46

The notation of w in the table includes its significant digits and the uncertainty of the last digit in parenthesis. If total N_{mc} test particles are simulated by TPMC in one case, and there are n_{ab} particles are absorbed by the active surfaces, w is given by the ratio

$$w = \frac{n_{ab}}{N_{mc}}. \quad (5)$$

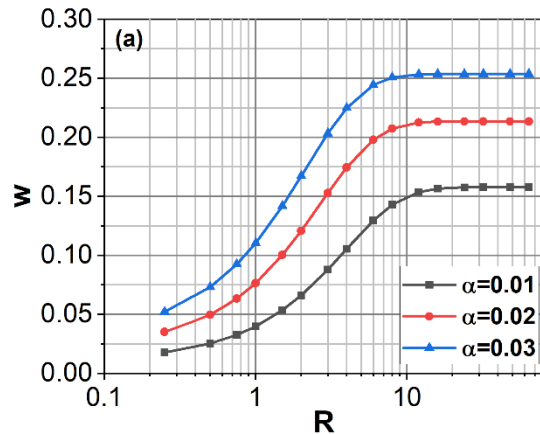
Because N_{mc} is a fixed number and only n_{ab} is of stochastic nature with statistical error, the variance (uncertainty) of w can be written as

$$\sigma(w) = \frac{\sigma(n_{ab})}{N_{mc}}, \quad (6)$$

and $\sigma(n_{ab})$ can be estimated by assuming a binominal distribution of the test particles in the simulation,¹⁰

$$\sigma(n_{ab}) \approx \sqrt{N_{mc}w(1-w)}. \quad (7)$$

We noticed that the pumping probability w of the reference cases without tube have very small deviations from the values of the initial sticking coefficients. This means that the conductance limitation of the short duct is negligible, and the improvement of the pumping probability comes from the self-replication procedure. In fact, the effect of the duct had also been checked if its length is 100 times shorter and the simulation results of w would only have a small relative change of a few percent in the positive direction. Moreover, it is found that for given sticking coefficient α , the increase of w is actually dependent on the active pumping area added in the system, which is the total area A of the tube walls. However, w will approach a maximum value as A increases. Because all tubes in each self-replication step N are identical in our simulation model, there exists a simple relationship between A/A_s and the length to diameter ratio of the tube R , i.e. $A/A_s = \pi R$. So w is actually determined by R , which has been proved by the simulation results in Table I.



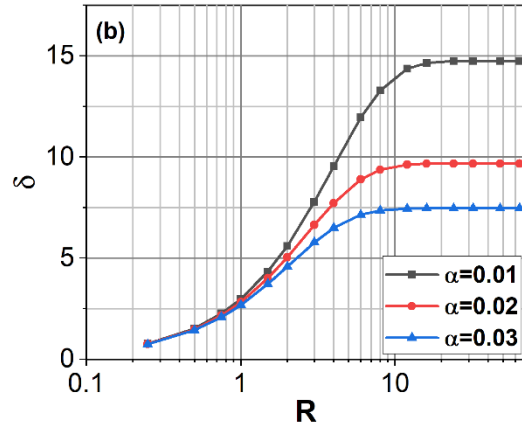


Fig. 3. System pumping probability (a) and its relative increase (b) versus R for different sticking coefficients α and diffuse reflection.

Figure 3 shows (a) the relation of w to R and α and (b) its relative increase δ . In the figures, $R=0$ corresponds to the original square with the pumping probability $w_0=\alpha$. It can be clearly seen that the maximum value of w depends on the original α , and the greater the original α is, the greater is the maximum value of w . However, the greater the original α is, the faster the relative increase will approach its maximum. In our cases, if the original $\alpha=0.01$, the maximum value of w is 0.1575, with a relative increase about $\delta=14.75$ times; if the original $\alpha=0.03$, the maximum value of w is 0.2536, with a relative increase about $\delta=7.46$ times.

Please note that the length of side of the original square could be arbitrary. This means that the pumping probability w of the system is determined by the ratio of the area of the tube walls to the area of the original square A/A_s . A larger original square is in favor of a higher pumping speed S and the tubes of larger diameters can be attached. But the effective w of the system is only determined by the ratio A/A_s (or R) after more and more active pumping surfaces are added, no matter how they would be arranged with fewer and longer tubes or with more and shorter tubes. This is reasonable if a smaller square is considered as one part of a larger original square. Moreover, this relationship would be the same if the tubes would be added with a different process other than the self-replication procedure in our study, for example, with $M=N^2$ ($N=1,2,3,\dots$).

The active pumping mechanism could be by condensation or cryosorption at cryogenic temperature for a cryogenic pump. This kind of cryogenic pumps has been used in nuclear fusion tokamaks.^{7-9,11-13} Another option is the NEG (Non-evaporable getter) material, which is widely used as the surface coating in large vacuum systems, such as the synchrotron,¹⁴⁻¹⁸ or to build a pump by cartridges that integrate many NEG disks on stacks.¹⁹⁻²¹ As demonstrated in this study, if the surface coating is after making holes of diameter 0.5 mm and length of 2 mm perpendicular to the surface, which can be easily realized with different mechanical processes or by lasers nowadays, the pumping probability could have a huge increase from initial $\alpha=0.01, 0.02, 0.03$ to $w=0.11, 0.17, 0.22$, respectively. And compared to the NEG cartridge, the self-replication structure proposed here can mitigate the disadvantage of the shadowing effect between NEG disks in the same cartridge. Because most applications of the gas absorption by NEG or of the cryogenic pumps are for the ultrahigh vacuum system, where the interaction between gas molecules is negligible, the simulation in free molecular flow regime by TPMC approach in this study is applicable.

Here we have only demonstrated the impact of this simple self-replication structure to the pumping probability. However, it has great application potentials related to many surface dominated processes, such as isotope separation by membrane²²⁻²³, hydrogen storage with high surface area²⁴⁻²⁵, heterogeneous catalysis²⁶, etc.

III. LIGHT ABSORPTION PROBABILITY

Topological effects in photonics have been studied in recent years.²⁷ Same simulation model in previous section will be used to study light absorption and reflection. Only α denotes the absorption rate instead of the sticking coefficient, and the diffuse reflection from active surface is replaced by the specular reflection for photons represented by the test particles in the simulation. Table II lists the simulation results of the absorption probability w of the system and corresponding relative increase $\delta = (w - \alpha)/\alpha$ of w .

TABLE II. The absorption probability w and corresponding relative increase δ by specular refraction.

	A	$\alpha=0.01$	δ	$\alpha=0.02$	δ	$\alpha=0.03$	δ
Reference case without tube	-	0.0099995(1)	-	0.0199978(1)	-	0.0299956(2)	-
N=1, M=1							
$T_L = 0.25a, R = 0.25$	$0.25\pi a^2$	0.0176064(1)	0.76	0.0348272(2)	0.74	0.0517234(2)	0.72
$T_L = 0.5a, R = 0.5$	$0.5\pi a^2$	0.0249301(2)	1.49	0.0487357(2)	1.44	0.0716517(3)	1.39
$T_L = 0.75a, R = 0.75$	$0.75\pi a^2$	0.0320230(2)	2.20	0.0619227(2)	2.10	0.0902082(3)	2.01
$T_L = a, R = 1$	πa^2	0.0389151(2)	2.89	0.0745025(3)	2.73	0.1076389(3)	2.59
N=2, M=4							
$T_L = 0.25a, R = 0.5$	$0.5\pi a^2$	0.0249283(2)	1.49	0.0487302(2)	1.44	0.0716417(3)	1.39
$T_L = 0.5a, R = 1$	πa^2	0.0389106(2)	2.89	0.0744882(3)	2.72	0.1076165(3)	2.59
$T_L = 0.75a, R = 1.5$	$1.5\pi a^2$	0.0521688(2)	4.22	0.0981066(3)	3.91	0.1396949(3)	3.66
$T_L = a, R = 2$	$2\pi a^2$	0.0648189(2)	5.48	0.1200027(3)	5.00	0.1687407(4)	4.62
N=3, M=16							
$T_L = 0.25a, R = 1$	πa^2	0.0389047(2)	2.89	0.0744721(3)	2.72	0.1075883(3)	2.59
$T_L = 0.5a, R = 2$	$2\pi a^2$	0.0648043(2)	5.48	0.1199668(3)	5.00	0.1686833(4)	4.62
$T_L = 0.75a, R = 3$	$3\pi a^2$	0.0885572(3)	7.86	0.1595826(4)	6.98	0.2196775(4)	6.32
$T_L = a, R = 4$	$4\pi a^2$	0.1105832(3)	10.06	0.1947462(4)	8.74	0.2633727(4)	7.78
N=4, M=64							
$T_L = 0.25a, R = 2$	$2\pi a^2$	0.0647870(2)	5.48	0.1199236(3)	5.00	0.1686132(4)	4.62
$T_L = 0.5a, R = 4$	$4\pi a^2$	0.1105430(3)	10.05	0.1946571(4)	8.73	0.2632439(4)	7.77
$T_L = 0.75a, R = 6$	$6\pi a^2$	0.1504009(4)	14.04	0.2548534(4)	11.74	0.3348326(5)	10.16
$T_L = a, R = 8$	$8\pi a^2$	0.1857919(4)	17.58	0.3049449(5)	14.25	0.3914363(5)	12.05
N=5, M=256							
$T_L = 0.25a, R = 4$	$4\pi a^2$	0.1104993(3)	10.05	0.1945553(4)	8.73	0.2630907(4)	7.77
$T_L = 0.5a, R = 8$	$8\pi a^2$	0.1856935(4)	17.57	0.3047559(5)	14.24	0.3911857(5)	12.04
$T_L = 0.75a, R = 12$	$12\pi a^2$	0.2463000(4)	23.63	0.3839095(5)	18.20	0.4752700(5)	14.84
$T_L = a, R = 16$	$16\pi a^2$	0.2967607(5)	28.68	0.4439364(5)	21.20	0.5346589(5)	16.82
N=6, M=1024							
$T_L = 0.25a, R = 8$	$8\pi a^2$	0.1856000(4)	17.56	0.3045622(5)	14.23	0.3909172(5)	12.03
$T_L = 0.5a, R = 16$	$16\pi a^2$	0.2965685(5)	28.66	0.4436189(5)	21.18	0.5342748(5)	16.81
$T_L = 0.75a, R = 24$	$24\pi a^2$	0.3763501(5)	36.64	0.5284776(5)	25.42	0.6116135(5)	19.39
$T_L = a, R = 32$	$32\pi a^2$	0.4369044(5)	42.69	0.5851316(5)	28.26	0.6586910(5)	20.96
N=7, M=4096							
$T_L = 0.25a, R = 16$	$16\pi a^2$	0.2964263(5)	28.64	0.4433548(5)	21.17	0.5339365(5)	16.80
$T_L = 0.5a, R = 32$	$32\pi a^2$	0.4366437(5)	42.66	0.5847502(5)	28.24	0.6582633(5)	20.94
$T_L = 0.75a, R = 48$	$48\pi a^2$	0.5223297(5)	51.23	0.6540155(5)	31.70	0.7103930(5)	22.68
$T_L = a, R = 64$	$64\pi a^2$	0.5795966(5)	56.96	0.6933475(5)	33.67	0.7370177(4)	23.57
N=8, M=16384							
$T_L = 0.25a, R = 32$	$32\pi a^2$	0.4384140(2)	42.84	0.5870841 (2)	28.35	0.6608203(1)	21.03
$T_L = 0.5a, R = 64$	$64\pi a^2$	0.5819109(2)	57.19	0.6959782(1)	33.80	0.7397407(1)	23.66
$T_L = 0.75a, R = 96$	$96\pi a^2$	0.6522725(2)	64.23	0.7366530(1)	35.83	0.7646180(1)	24.49
$T_L = a, R = 128$	$128\pi a^2$	0.6922547(1)	68.23	0.7559609(1)	36.80	0.7753285(1)	24.84
N=9, M=65536							
$T_L = 0.25a, R = 64$	$64\pi a^2$	0.5819129(5)	57.19	0.6959789(5)	33.80	0.7397433(4)	23.66
$T_L = 0.5a, R = 128$	$128\pi a^2$	0.6922541(5)	68.23	0.7559609(1)	36.80	0.7753275(4)	24.84
$T_L = 0.75a, R = 192$	$192\pi a^2$	0.7335582(4)	72.36	0.7728623(4)	37.64	0.7840044(4)	25.13
$T_L = a, R = 256$	$256\pi a^2$	0.7531902(4)	74.32	0.7797314(4)	37.99	0.7873112(4)	25.24

The notation of w in Table II is same as in Table I, and the uncertainties in the parentheses are estimated by Eq. (7). From the simulation results we know that many conclusions in previous

section hold. However, quantitatively, the specular reflection boundary condition has greater effect to the improvement of w as shown in Figure 4.

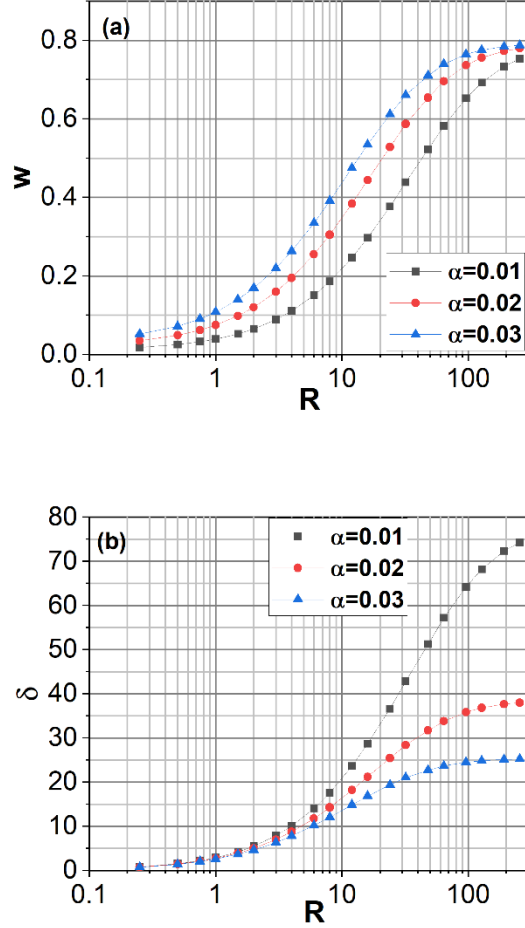


Fig. 4. System absorption probability (a) and its relative increase (b) versus R for different absorption rates α and specular reflection.

Compared to the diffuse reflection, we can see that the improvement of w will approach the maximum much slower when the boundary condition is changed to the specular reflection. In our simulation example, the ultimate absorption probability w of the system is given by Eq. (4) by assuming $w_{\text{tube}}(\alpha)=1$, which is $w=0.7875$, 0.7897 , 0.7918 for $\alpha=0.01$, 0.02 , 0.03 , respectively. It can be seen from the simulation results that for the specular reflection, the maximum values of w can approach the ultimate values as A/A_s or R increases. This implies that $w_{\text{tube}}(\alpha)$ will approach unity (black body) and is only limited by the normal incident photons from the light source.

In practice, there is no difficulty to make four million holes of diameter of 0.1 mm and length of 3.2 mm in the original square of $a = 200$ mm, and the absorption probability w of the system could have a huge increase from initial $\alpha=0.01, 0.02, 0.03$ to $w=0.44, 0.59, 0.66$, and corresponding relative increase of w is 43 times, 28 times, 21 times, respectively. The diameter of 0.1 mm is still much larger than the wavelength of light λ , if λ is 600 nm. Under this condition, to calculate the absorption probability by the test particle Monte Carlo simulation without taking the wave diffraction into account would be applicable.²⁸⁻³⁰ Obviously, the significant improvement of the system absorption probability by such a simple self-replication geometric structure has great application potential in solar cells if it could be compatible with the need to collect the electrical charges, or in converting the solar irradiation into heat through the collector fluid. Moreover, because the reflection probability of the system is $1-w$, this self-replication geometric structure would be useful to reduce the detection possibility of stealth aircrafts and boats.

In the simulation, the photons (test particles) are coming from a uniform diffuse light source. If the light is normal incidence, the absorption probability remains as α ; if it comes from a special incident angle, the result could be different, and is possible to be studied with our simulation model in near future.

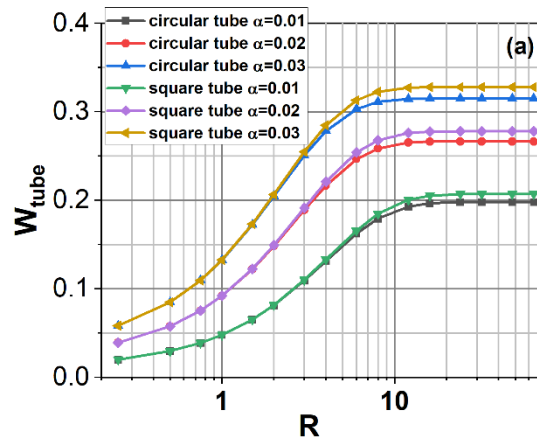
IV. MORE COMPLICATED SYSTEM

As said, if all tubes in each self-replication step N are independent and identical, the effective pumping probability or the absorption probability of the system can be calculated by Eq. (4). Using this method, only the simulation of $w_{\text{tube}}(\alpha)$ is needed.

Furthermore, the system in the study is created principally by extruding the circles enclosed by the original squares into a bundle of parallel tubes in the third perpendicular direction. Because only the performance of the tubes has changed, it would be reasonable to reduce the remaining flat

area with unchanged performance as much as possible. One possible method to do that is to use tubes of square cross section instead of tubes of circular cross section.

Fig. 5 shows the simulation results and comparisons of the pumping probability and the absorption probability of these two kinds of tubes, under diffuse and specular reflections, respectively. Here, R represents the ratio of length to diameter for the circular tube, and the ratio of tube length to square side length for the square tube, respectively. It can be also clearly seen that the final approached maximum value of w depends on the original α , and the greater the original α is, the greater is the maximum value of w . Moreover, the maximum values of w are less than unity under diffuse reflection condition, but w will approach unity under specular reflection condition. In addition, compared to the circular tube under diffuse reflection, if the tube is long enough, the maximum values of the pumping probability of the square tube are 4.6% to 4.1% higher for α ranging from 0.01 to 0.03. When the diffuse reflection is replaced by the specular reflection, the absorption probability of the square tube is also higher than that of the circular one by up to 3%.



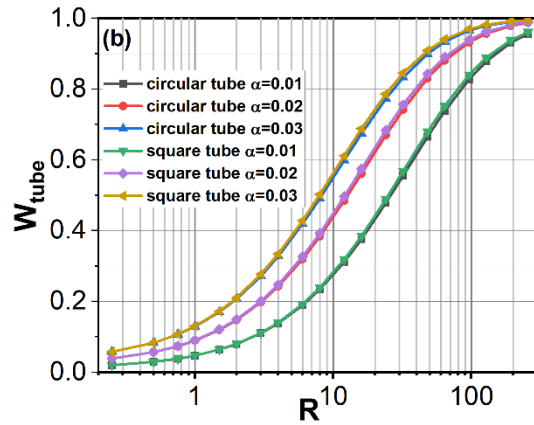


Fig. 5. Pumping probability under diffuse reflection (a) and absorption probability under specular reflection (b) of two different tubes versus R for different sticking coefficients (absorption rates) α .

Up to now, the ideal case of no distance between the walls of the adjacent tubes is considered. In this case, the space between the tubes could be used for the installation of necessary heating elements for NEG regeneration or electrodes to collect the electricity, or reserved to hold the collector fluid in converting the solar irradiation energy into heat. Actually, it would be more realistic to have a distance between the walls of the adjacent tubes, and Eq. (4) should be modified by using different weighting factors k_1 and k_2 for $w_{\text{tube}}(\alpha)$ and α instead of $\pi/4$ and $(1 - \pi/4)$. For example, if making one million circular holes of diameter of 0.1 mm and length of 3.2 mm in the original square of $a = 200$ mm and the distance between adjacent holes about 0.1 mm, and the weighing factor of the opening area for the light is $k_1=0.19635$. In such a case, the photon absorption probability w of the system under specular reflection could have an increase from initial $\alpha=0.01, 0.02, 0.03$ to $w=0.117, 0.162, 0.188$. If the circular tubes are replaced by the square tubes and the square side length is also 0.1 mm, the corresponding photon absorption probability w of the system will increase to $w=0.150, 0.204, 0.234$ from $\alpha=0.01, 0.02, 0.03$, respectively. This further increase is mainly because of larger weighing factor of the opening area for the light $k_1=0.25$, which is 27% bigger compare to that for the circular tubes.

In order to exploit the topological effect in the design of a NEG pump and a cryogenic pump, the relationship between the maximum value of w_{tube} of a circular tube and the sticking coefficient α under diffuse reflection and corresponding length to diameter ratio R when w_{tube} reaches 95% of its maximum value are given in Fig. 6 (a) and (b), respectively.

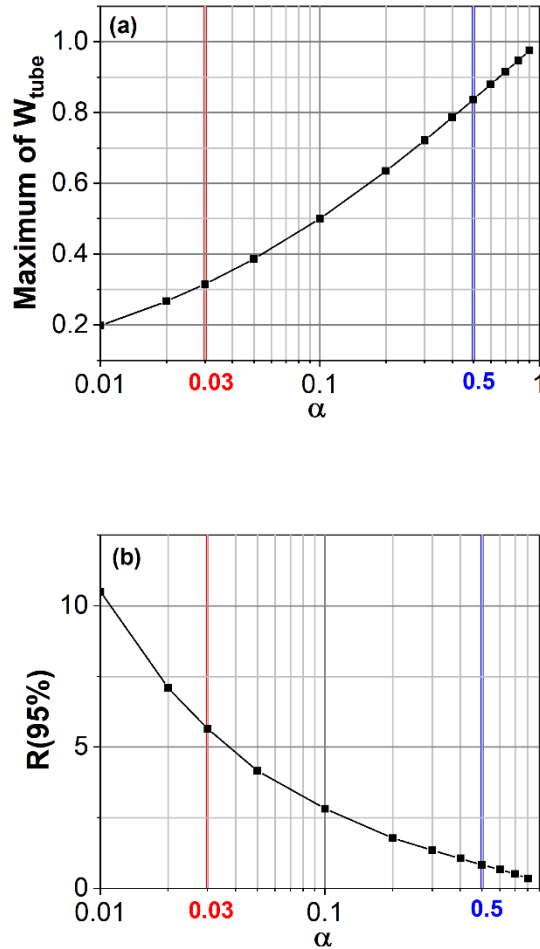


Fig. 6. Maximum of w_{tube} under diffuse reflection (a) and the corresponding R when w_{tube} reaches 95% of the maximum (b) of a circular tube versus the sticking coefficient α .

It can be seen that for large α , the maximum value of w_{tube} will approach unity when the tube is long enough. At a given diameter, the length of the tube needed for w_{tube} to reach 95% of its maximum value becomes shorter as α increases. In addition, as marked in the figure, the nominal sticking coefficient α of the NEG material usually ranges from 0.01 to 0.03,¹⁷ and that of the

charcoal coated surface at cryogenic temperature is above 0.5 depending on the gas species.³ It is seen from Fig. 6 that the benefit, i.e. the relative increase of the pumping probability of the topological structures is bigger for the NEG material. From the datasheets of commercial NEG pumps and our experience,²⁰⁻²¹ the pumping probability of the NEG pump based on the cartridge structure is less than 0.25 for hydrogen. However, the topological structures provide us an alternative NEG pump design approach, and it would be possible to increase the pumping probability to 0.3 by the square NEG tubes with small distances as shown in Fig. 5(a). More important, the topological structures will greatly improve the pumping ability of NEG coated surfaces.

If the system is more complicated and the tubes are not independent of each other, it could be directly simulated. As shown in Table II, the system of 65536 tubes has been directly and successfully simulated, and in principle, each tube could have individual physical and geometric parameters. In addition, because the code ProVac3D has a speed-up efficiency of more than 80% with 16000 cores for parallelization, huge numbers of test particles can be simulated, and the results in this paper are of high statistical precision.

V. SUMMARY AND CONCLUSIONS

Usually, the requirement of the vacuum pumping is to provide high pumping speed for given gas load under the system geometric constraint. It is found that under the area constraint of the original square, the topological features of a simple two dimensional self-replication structure can be exploited by adding tubes in the third perpendicular dimension and the pumping probability of the system can be significantly improved. When the diffuse reflection on surfaces for gas molecules is replaced by the specular reflection for photons, the improvement of the light absorption probability of the system is even greater. Furthermore, the relationship to the geometric

and physical parameters and corresponding maximum values of the system pumping / light absorption probability have been obtained by systematic Monte Carlo simulations.

The study in this paper proposes a novel and simple way to achieve better system performance of the pumping probability or the light absorption probability under the geometric constraint and with relatively poor surface pumping sticking coefficient or photon absorption rate. So the results have a great potential for different applications such as in vacuum pumping, in photovoltaic industry and by converting the solar irradiation energy into heat.

Analogue to the cases originated from a two dimensional self-replication structure studied in this paper, a three-dimensional structure produced by the self-replication process of a cube with an enclosed sphere has good features that the sum of spheres' surface area can increase as the sum of their volumes remains as the same. One potential application to batteries could increase energy storage density, which is essential for electric cars, assuming that battery storage capabilities are related to the surface area available inside the battery.

ACKNOWLEDGMENTS

We acknowledge EUROfusion for the computation resources allocated to project VAC_ND to run high performance computer Marconi Fusion at Cineca, Italy.

DATA AVAILABILITY

The data that support the findings of this study are available from the corresponding author upon reasonable request.

REFERENCES

- ¹ M. Nakahara, *Geometry, topology and physics*, 3rd edition (Taylor & Francis, 2021).
- ² S. M. Carroll, *Spacetime and geometry: An Introduction to General Relativity* (Cambridge University Press, 2019).
- ³ *Handbook of Vacuum Technology*, 2nd Edition, edited by K. Jousten (John Wiley & Sons, 2008).
- ⁴ R. Kersevan and J.-L. Pons, *J. Vac. Sci. Technol. A* **27**, 1017 (2009).

- ⁵ <https://molflow.web.cern.ch/>
- ⁶ X. Luo and Chr. Day, *J. Vac. Sci. Technol. A* **26**, 1319 (2008).
- ⁷ X. Luo, Chr. Day, H. Haas, and S. Varoutis, *J. Vac. Sci. Technol. A* **29**, 041601 (2011).
- ⁸ X. Luo and Chr. Day, *Fusion Engineering and Design* **85**, 1446 (2010).
- ⁹ X. Luo, M. Scannapiego, Chr. Day, and S. Sakurai, *Fusion Engineering and Design* **136**, 467 (2018).
- ¹⁰ Y. Suetsugu, *J. Vac. Sci. Technol. A* **14**, 245 (1996).
- ¹¹ M. Glugla, D. K. Murdoch, A. Antipenkov, S. Beloglazov, I. Cristescu, I.-R. Cristescu, C. Day, R. Laesser, A. Mack, *Fusion Engineering and Design* **81**,733 (2006).
- ¹² V. Kalinin, E. Tada, F. Millet, N. Shatil, *Fusion Engineering and Design* **81**, 2589 (2006).
- ¹³ C. Day, D. Murdoch, R. Pearce, *Vacuum* **83**, 773-778 (2008).
- ¹⁴ C. Benvenuti, P. Chiggiato, F. Cicoira, and Y. L'Aminot, *J. Vac. Sci. Technol. A* **16**, 148 (1998).
- ¹⁵ C. Benvenuti, J. M. Cazeneuve, P. Chiggiato, F. Cicoira, A. E. Santana, V. Johaneck, V. Ruzinov, J. Fraxedas, *Vacuum* **53**, 219 (1999).
- ¹⁶ P. Chiggiato, P. C. Pinto, *Thin Solid Films* **515**, 382 (2006).
- ¹⁷ C. Benvenuti, P. Chiggiato, P. Costa Pinto, A. Escudeiro Santana, T. Hedley, A. Mongelluzzo, V. Ruzinov, I. Wevers, *Vacuum* **60**, 57 (2001).
- ¹⁸ Ch. Day, X. Luo, A. Conte, and P. Manini, *J. Vac. Sci. Technol. A* **25**, 824 (2007).
- ¹⁹ Y. Li, D. Hess, R. Kersevan, and N. Mistry, *J. Vac. Sci. Technol. A* **16**, 1139 (1998).
- ²⁰ <https://www.saesgetters.com/>
- ²¹ X. Luo, L. Bornschein, Ch. Day, and J. Wolf, *Vacuum* **81**, 777 (2007).
- ²² T. Hoshino, T. Terai, *Fusion Engineering and Design* **86**, 2168 (2011).
- ²³ M. Hankel, Y. Jiao, A. Du, S. K. Gray, and S. C. Smith, *J. Phys. Chem. C* **116**, 6672 (2012).
- ²⁴ H. Kabbour, T. F. Baumann, J. H. Satcher, A. Saulnier, and C. C. Ahn, *Chem. Mater.* **18**, 6085 (2006).
- ²⁵ D. Portehault, C. Giordano, C. Gervais, I. Senkovska, S. Kaskel, C. Sanchez, M. Antonietti, *Adv. Funct. Mater.* **20**, 1827 (2010).
- ²⁶ J. M. Thomas, W. J. Thomas, *Principles and Practice of Heterogeneous Catalysis*, 2nd Edition (Wiley-VCH, 2015).
- ²⁷ T. Ozawa, H. M. Price, A. Amo, N. Goldman, M. Hafezi, L. Lu, M. C. Rechtsman, D. Schuster, J. Simon, O. Zilberberg, and I. Carusotto, *Rev. Mod. Phys.* **91**, 015006 (2019).
- ²⁸ J. R. Mahan, *Radiation Heat Transfer – A Statistical Approach* (John Wiley & Sons Inc., 2002).
- ²⁹ J. R. Howell, M. P. Mengüç, K. Daun, R. Siegel, *Thermal Radiation Heat Transfer*, 7th edition (Taylor & Francis/CRC, 2021).

³⁰ X. Luo, V. Hauer, and Chr. Day, Fusion Engineering and Design **87**, 603 (2012).

Tables

TABLE I. Simulation results of the pumping probability w and corresponding relative increase δ .

TABLE II. The absorption probability w and corresponding relative increase δ by specular reflection.

Figure captions

Fig. 1. The self-replication in the first steps from $N=1$ to $N=3$.

Fig. 2. The potential to exploit the dimension perpendicular to the plane in the first step $N=1$.

Fig. 3. System pumping probability (a) and its relative increase (b) versus the sticking coefficient and R .

Fig. 4. System absorption probability (a) and its relative increase (b) versus the absorption rate and R .

Fig. 5. Pumping probability under diffuse reflection (a) and absorption probability under specular reflection (b) of two different tubes versus the sticking coefficient or absorption rate α and R .

Fig. 6. Maximum of w_{tube} under diffuse reflection (a) and the corresponding R when w_{tube} reaches 95% of the maximum (b) of a circular tube versus the sticking coefficient α .